JOURNAL OF CATALYSIS 64, 213–222 (1980)

Characterization of Small Platinum Particles Supported on Graphite by Electron Microscopy

M. JOSÉ YACAMÁN* AND J. MANUEL DOMINGUEZ E.†

* *Instituto de Física, UNAM, Apartado Postal 20-364, México 20, D.F., and † Instituto Mexicano del Petróleo, Avenida de los 100 Metros 152, México 14, D.F., Mexico*

Received April 10, 1979; revised August 13, 1979

Characterization of small platinum particles in the Pt/graphite catalyst is done using high-resolution dark-field electron microscopy and single-particle electron diffraction. Two types of hexagonal-shaped particles were found. Both are shown to correspond to a three-dimensional cubo-octahedral shape. The first type has a (111) face in contact with the (0001) face of the graphite surface. The second type has a (110) face parallel to the (0001) face of the support surface. The faceted Pt particles are bounded by (100) and (111) crystallographic planes, which provide specific sites for a catalytic reaction.

1. INTRODUCTION

The shape and crystallography of small metallic particles seem to play an important role in the properties of supported metal catalysts (*1–5*). Indeed, some special configurations on the surface of particles could influence the catalytic activity for certain reactions (*2, 6*). However, it is not always possible to characterize both shape and crystallography because the high dispersion of metal in the carrier makes difficult the application of standard transmission electron microscopy techniques in particular. In spite of these limitations some recent works have shown interesting features about the morphology of particles and their interaction with the support. Baker *et al.* (*7*) and Chen and Schmidt (*8*) have observed for Pt/TiO_2 and Pt/amorphous silica systems, respectively, that in some cases the particles appear to have a hexagonal outline. In the former case the particles are reported to have a pillbox shape. Chen and Schmidt pointed out that about 20% of the particles present contrast features which might be associated with single twinning. On the other hand only a small fraction of the particles show the typical contrast of multiply twinned particles (*9*). All these results are in contrast with earlier work using intermediate-resolution microscopy in which spherical particle shapes were reported (*10, 11*). Faceted hexagonal particles have been observed in other interesting systems like Pt–Pd (*12*) and Rh in Al_2O_3 (*13*).

Characterization of the support as well as of the metal is very important in order to define their interaction (*7*). In this work high-resolution TEM and microdiffraction techniques have been applied to the characterization of the shape and crystallography of small metal particles for the Pt/graphite catayst. The weak-beam dark-field technique developed by Yacamán and Ocaña (*14*) was used to determine the three-dimensional shape of the particles. High-resolution techniques were also applied to the support characterization. The results obtained by these methods have been used to interpret the kinetic data obtained in the neopentane conversion on the Pt/C catalyst, reported in the second part of this work (*21*).

2. EXPERIMENTAL METHODS

(*a*) *Sample Preparation*

The preparation of Pt/C catalyst was made using materials of high purity. The support was a graphite LONZA-LT10, type

0021-9517/80/070213-10$02.00/0

ex-anthracite, with 99.9% carbon, as reported by the supplier. The surface area determined by BET adsorption of N_2 equals 18 m^2/g and the density equals 2.2 g/cm^3. The metal, Pt, was deposited on the support from chloroplatinic acid (H_2PtCl_6, $6H_2O$) using the method of Bartholomew and Boudart (*15*). This consists of the impregnation of graphite with a solution of the metallic compound in a mixture of ethanol and benzene, in the proportion 1 to 4, respectively. The 10% (wt) Pt/C catalyst was obtained from a solution of 10 ml of ethanol and 1 g of support. The mixture was shaken for 24 hr and then the excess of solvent was eliminated by heating the powder at 60°C in an evaporator for several hours. The sample was then dried in air at 80°C for 12 hr in an oven. The obtained powder was placed in a quartz cell and heated at 850°C in the presence of a hydrogen flow. Thus the sample was left 16 hr in a static atmosphere of hydrogen and then was purged with argon (99.99%) until room temperature was reached.

(*b*) *Electron Microscopy*

Samples were mounted on 200-mesh grids covered with a layer of carbon which was evaporated from standard electrodes at a vacuum of 10^{-6} Torr. The Pt/C powder was ultrasonically dispersed in ethanol and mounted on the grid, where a drop of the suspension was then air dried.

Observation were carried out in a JEOL 100-C electron microscope fitted with a high-resolution top-entry goniometer stage. Tilting of the sample proved to be most important in finding the best orientation for visibility of small metallic particles. Dark-field images were obtained by tilting the

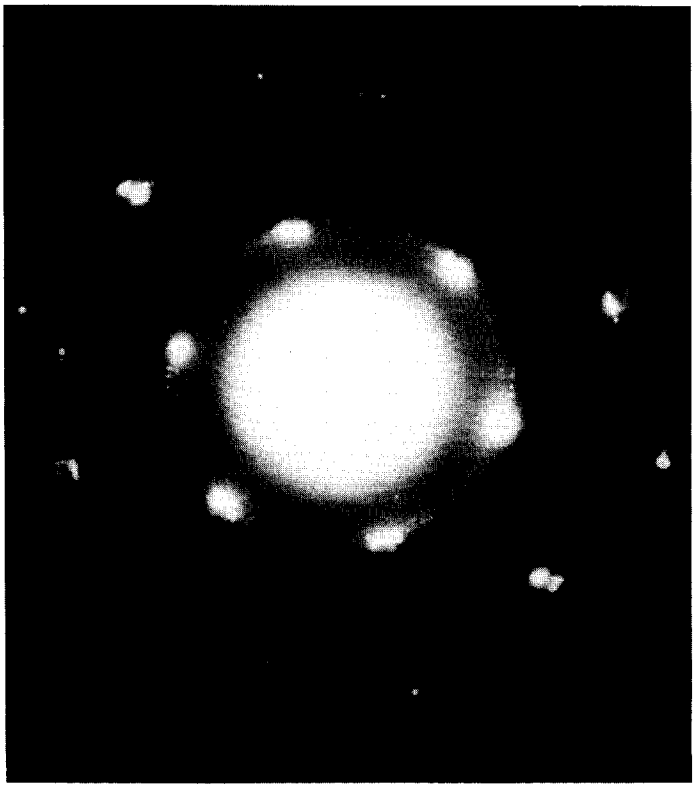

FIG. 1. Diffraction pattern of the graphite support showing the ⟨0001⟩ zone axis.

electron beam so as to make the diffraction spot spatially coincident with the current center of the microscope. Astigmatism was corrected using the phase-contrast features of the carbon film. The rotation between the image and the diffraction pattern was calibrated using Mn_2O_3 whiskers. Lattice images of the same whiskers were used to calibrate the magnification.

3. RESULTS

(*a*) *Characterization of the Support*

The electron diffraction patterns of graphite were obtained for a 1-μm-diameter support region. Figure 1 shows the pattern corresponding to the $\langle 0001 \rangle$ zone axis where the characteristic hexagonal symmetry can be observed. All the spots were split into several subspots because within each grain there were often several subgrains rotated with respect to each other. This result was confirmed by the observation of interference (Moiré) fringes produced by the azimuthally rotated grains. Figure 2 shows the fringe pattern which is obtained by allowing passage of two diffracted spots ($\mathbf{g}_1$, $\mathbf{g}_2$ vectors) by the objective aperture. It has been verified that there exists a periodicity given by

$$d = 1/\Delta\mathbf{g}.$$

The direction of the fringes is normal to $\mathbf{g}$. For instance the fine fringes (9.4 Å) in Fig. 2 are produced by the interference of two (1010) reflections rotated by 13°. In addition we can observe a larger periodicity (~72 Å) produced by the interference of a beam with another double-diffracted beam. On the other hand, when a single spot contributed to form the dark-field image a large area (1 to 2 μm) appeared bright. These results indicate the strong crystalline character of the support. The particles are grown in contact with a large monocrystalline substrate portion. No evidence was found of formation of long channels on the graphite produced by methanation of the

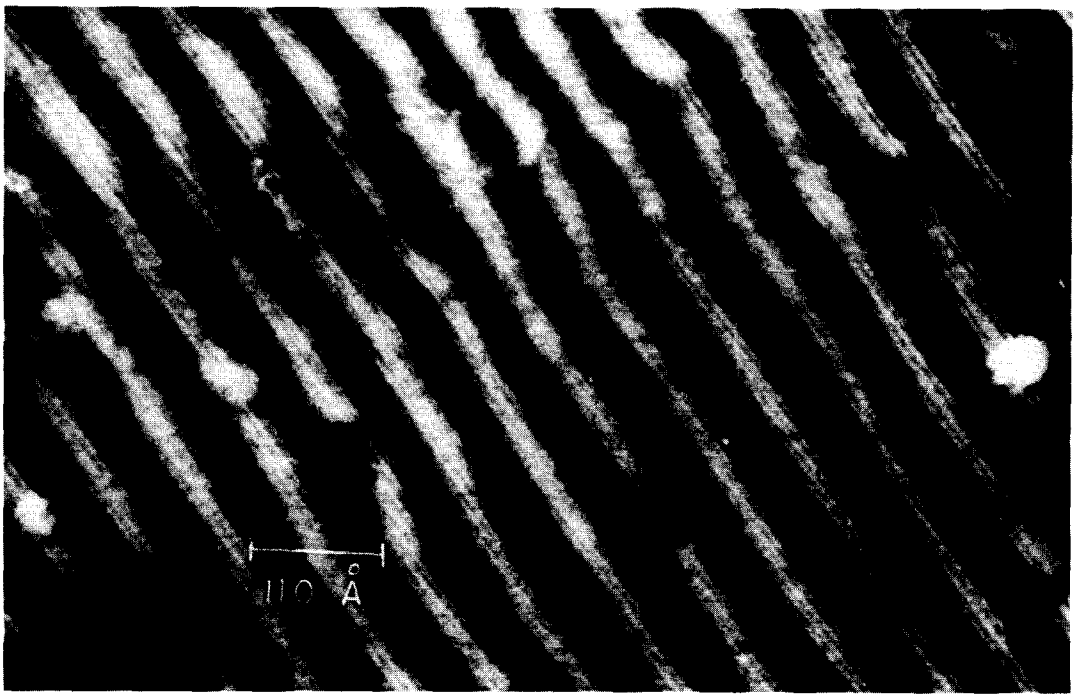

FIG. 2. Dark-field images of graphite showing a fine periodicity of 9.4 Å and a large one of ~72 Å.

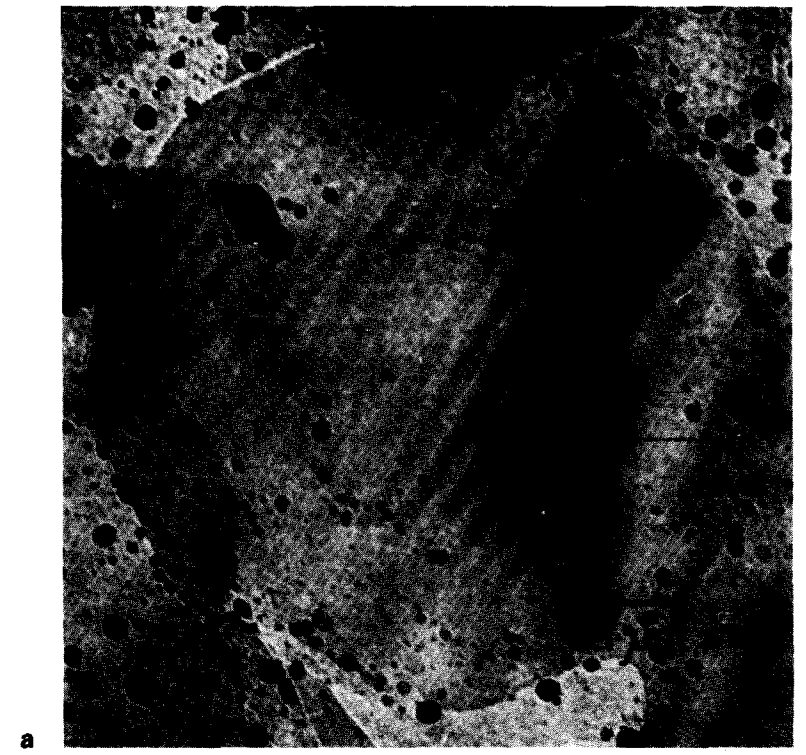

a

b

FIG. 3. Tilting sequence of a Pt/graphite catalyst showing the dependence of the particle visibility on substrate orientation. (a) Bright field. (b) (111) Pt dark field with a near-(1010) graphite reflection

c

d

strongly excited. (c) Same Pt reflection with the support tilted by 1° out of the Bragg condition for the same (1010) reflection. (d) Support tilted by 2°. (e) Same image when the support is completely out of contrast. Note the faint particle contrast.

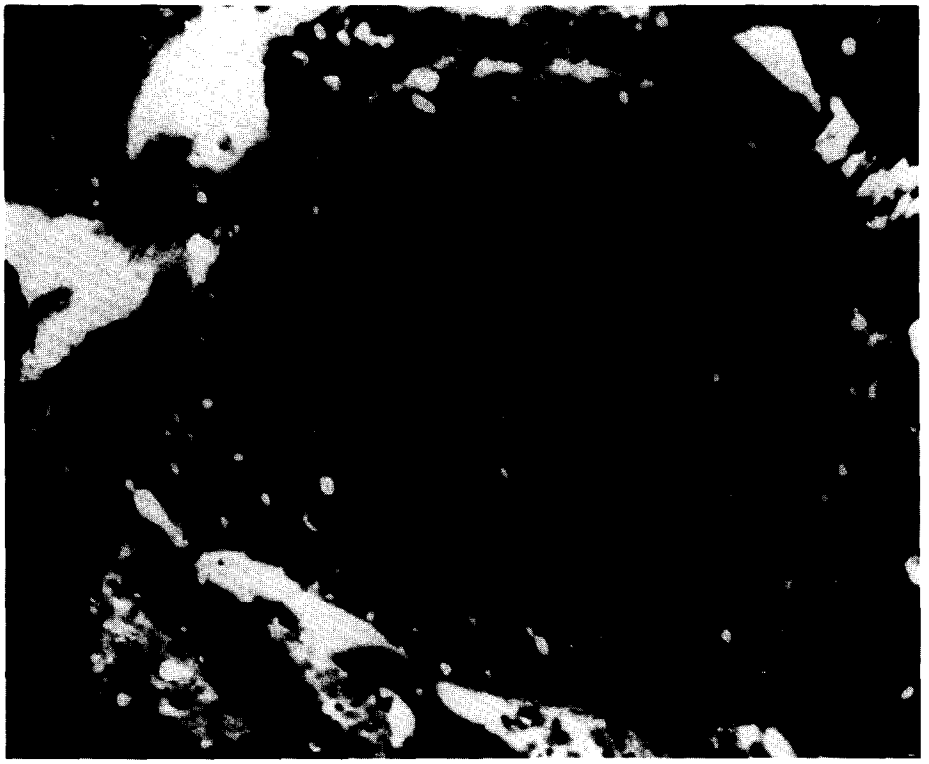

e

FIG. 3—*Continued*

carbon (*7*). Damage of this kind would have shown up as a disturbance on the Moiré patterns. However, in some areas, pitting localized around very large particles was found, indicating that some methanation was probably taking place on the surface (*7*).

(*b*) *Visibility of the Pt Particles*

The contrast of small metallic particles is strongly dependent upon the orientation of the crystalline substrate. This is especially true for the dark-field images. Figure 3 shows a tilting sequence of the sample. Figure 3a corresponds to the bright-field image showing well-faceted hexagonal particles. some of the Pt particles produce (111) reflections and dark-field images can be formed by using such reflections. This type of image is presented in Figs. 3b to e as a function of substrate orientation. In Fig. 3b the substrate is near the Bragg condition (strongly diffracting), and the particles are not visible. A similar situation is produced when the substrate is completely out of the diffraction condition (Fig. 3e). The best visibility conditions are produced for some orientation of the sample which corresponds to tilting angles between 1 and 2° from the Bragg angle (Figs. 3c and d). This sequence shows that the best condition for particle observation must be found on an individual basis. It is clear that the number of particles visible by dark field is always less than that observed in bright field (at least for the case described here). A similar conclusion was reached by Freeman *et al.* (*17*) for the Pd/Al_2O_3 system using selected-zone dark-field images.

Figure 3 demonstrates that a tilting sequence is required for best dark-field set-

ting. Frequently the particle will be out of contrast and a tilting would be necessary for proper observation.

(c) *Diffraction and Contrast of Pt Particles*

The diffraction pattern of a catalyst area containing a large number of platinum particles is shown in Fig. 4. Besides the graphite reflections the (111), (200), (242), and (422) platinum reflections were identified.

Two main types of particles were visible on the bright-field image. The first, shown in Fig. 5a, corresponds to particles with a hexagonal profile, and the second, shown in Fig. 5b, are particles with elongated hexagonal profiles. Hereafter these particles will be called H_1 and H_2, respectively.

In dark-field images, particles of type H_1 were only visible on the (220) and (242) reflections without considering orders higher than this one. H_2 particles on the other hand were visible in (111), (200), and (220) reflections. Typical dark-field images for both particles are shown in Figs. 5c and d. As can be observed, the hexagonal profile is retained in both cases. That indicates that the diffracting planes are continuous along the particle and shows that the particles are single crystals and not multiply twinned hexagonal particles which will have profiles in dark field showing the hexagonal profile partially (because not all the crystal planes are continuous along the particle).

In Fig. 6 a microdiffraction pattern of an individual H_2 particle with a mean size of about 100 Å is shown. This pattern was obtained using the STEM attachment for

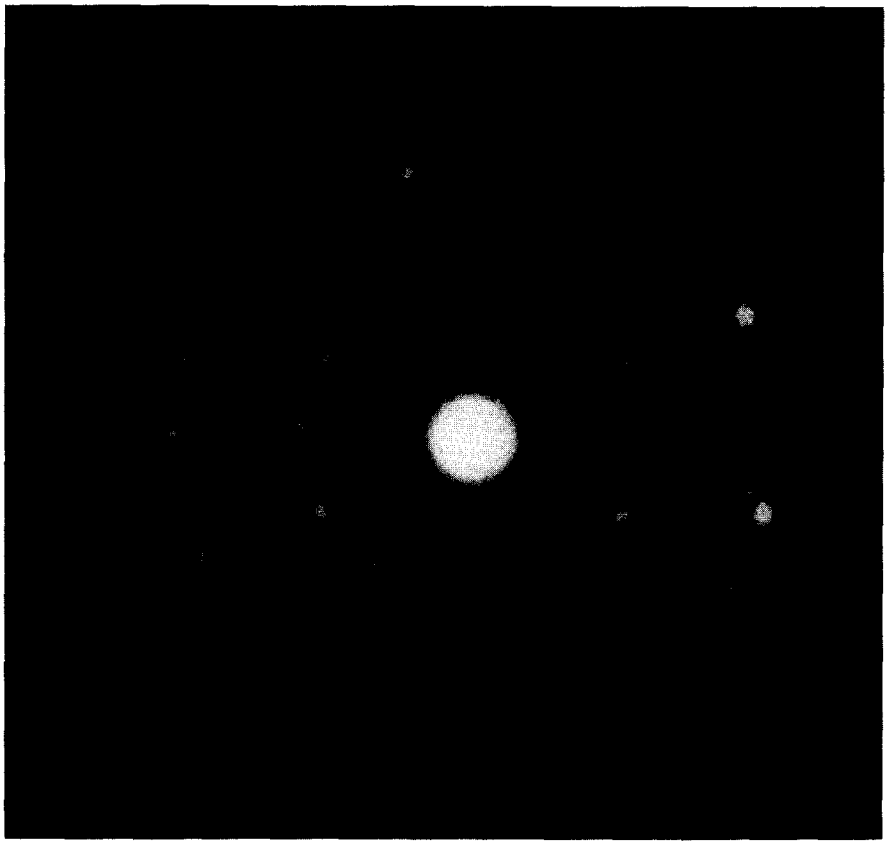

FIG. 4. Diffraction pattern of a catalyst region containing a large number of Pt particles.

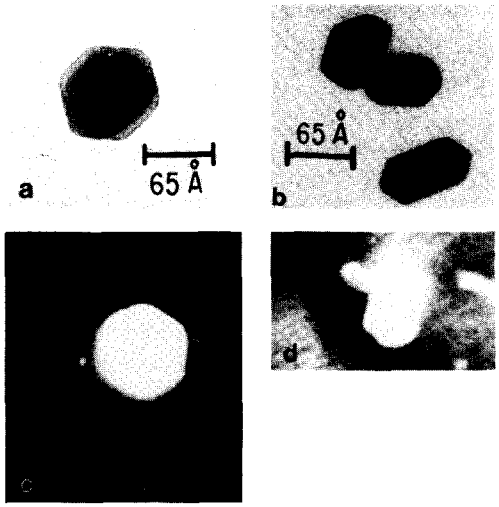

FIG. 5. Different types of particles observed in a Pt/C catalyst. (a) Bright field of hexagonal particle (H_1). (b) Bright field of several elongated hexagonal particles (H_2). (c) (220) Dark-field image of a H_1 particle. (d) (111) Dark-field image of a H_2 particle.

the JEOL 100-CX microscope. The pattern contains reflections of Pt and graphite and can be indexed as produced by a fcc crystal in a ⟨110⟩ zone axis. Similar patterns for the H_1 particles were indexed as belonging to a ⟨111⟩ zone axis. From these patterns it was confirmed that Pt particles have a single-crystal character and they retain the fcc bulk crystal symmetry. Moreover those single-particle patterns found were very similar to those computed by Larroque and Brieu (*19*) for cubo-octahedral fcc crystals.

4. DISCUSSION

The experimental diffraction and dark-field data obtained in our work can be explained by assuming that the shape of the particle is cubo-octahedral. The H_1 particles have a (111) plane in contact with the (0001) graphite surface and the H_2 particles have a (110) plane in contact with the same surface.

With respect to the H_1 particle there are two possible three-dimensional shapes that could give a hexagonal profile when projected along a ⟨111⟩ axis and have the correct diffracting planes: the octahedron and the cubo-octahedron. When an image is formed using a (220) spot the projected images of an octahedron and of a cubo-

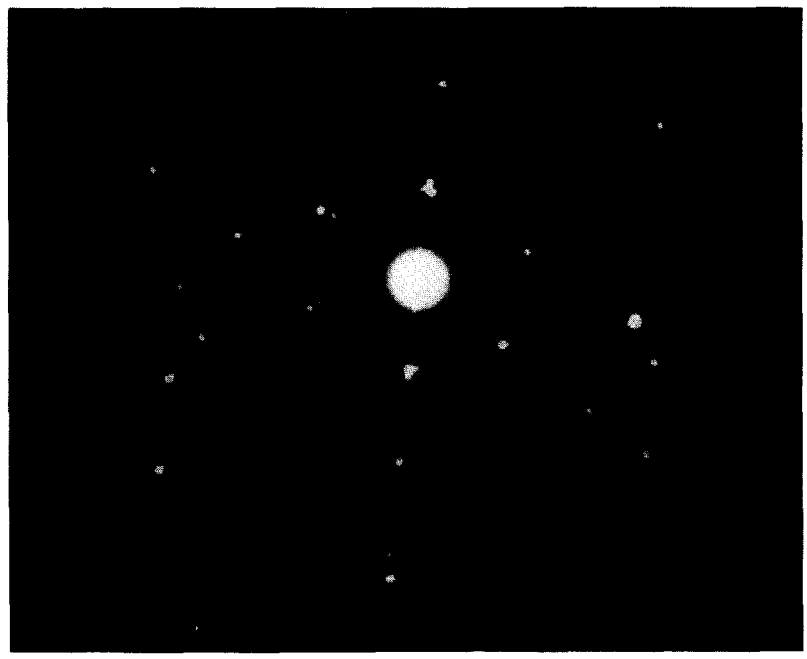

FIG. 6. Microdiffraction pattern of a H_2-type single particle.

octahedron are oriented differently with respect to the operating **g** vector as shown in a previous paper (*20*). After calibration of the image diffraction patterns we can use the relative orientation of the dark-field images to distinguish between these two possibilities. Figure 7 shows an actual experimental picture in which the orientation of the image with respect to the **g** vector confirmed that the particles are fcc cubo-octahedrons. Thickness fringes were occasionally observed in large particles which also happen to be located on thin substrate areas. Those fringes give a direct indication of the particular shape (*14*). An example for H_2-type particles is shown in Fig. 8b where the fringes have exactly the profile predicted by the cubo-octahedron model.

By using the thickness fringes in Fig. 8 and the value of the extinction distance obtained from dynamical diffraction theory it is estimated that the height of the particle in Fig. 8 was about 80 Å. However, it should be noted that the particle in Fig. 7 shows only one thickness fringe. This indicates that some of the particles may have the shape of a truncated cubo-octahedron and might correspond to the case reported by Baker *et al.* (*7*). We found no evidence of multiply twinned particles (*18*). This indicates the strong nature of the interaction between metal particles and the graphite.

It is interesting to remark that we had not observed channeled surfaces of graphite as reported previously by some authors (*7, 22 23*). Channeling is assumed to originate from methanation of the carbon surface during the migration of metal particles. Thus methanation could occur near the Pt/graphite interface at high temperatures (~600°C) as reported elsewhere (*22–25*). The high crystalline character of our support and the absence of pronounced defects could eventually limit the formation of deep channels on the surface (*24*).

5. CONCLUSIONS

The Pt/graphite catalyst has been characterized using weak-beam dark-field and microdiffraction techniques. It was found that the support is highly crystalline and is made of overlapping mosaics which are rotated with respect to each other. The platinum particles have a three-dimensional shape corresponding to a cubo-octahedron which sometimes might be truncated. Particles of type H_1 have a (111) face in contact with the (0001) graphite surface. Particles

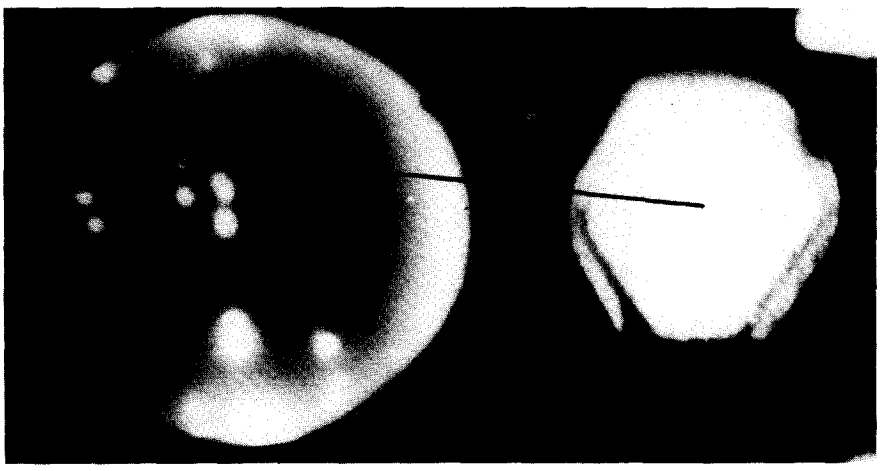

FIG. 7. Composite picture showing the relation between the orientation of the (220) dark-field image of a H_1 hexagonal particle and the **g** vector of the operating reflection. This orientation can only be achieved by a cubo-octahedron.

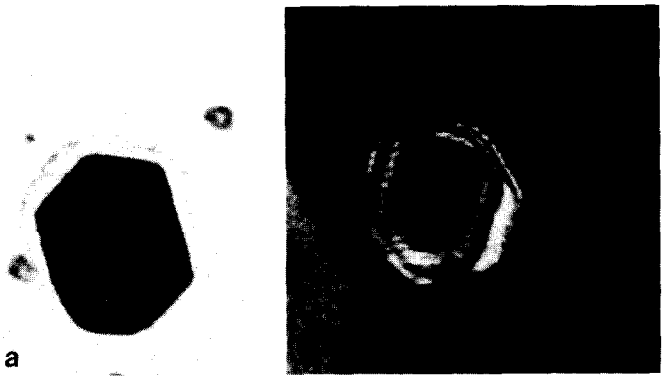

FIG. 8. Image of a H_2-type particle. (a) Bright field. (b) (111) Dark field showing thickness fringes that confirm the cubo-octahedral shape.

of type H_2 have a (110) face in contact with the same graphite surface.

In both caes the faces exposed by the particles to reactive gas in a catalytic reaction are the (111) and (100) faces. In the following paper this characterization will be applied to the study of the neopentane conversion.

ACKNOWLEDGMENTS

The microdiffraction pattern was obtained in a JOEL 100-CX STEM microscope in JEOL Laboratories. We are indebted to Mr. F. Ruíz for technical help and to Drs. D. Romeu, A. Gómez, S. Fuentes, and J. Zenith for useful discussions.

REFERENCES

1. Van Hardeveld, R., and Hartog, F., *Surface Sci.* **15**, 189 (1969).
2. Van Hardeveld, R., and Van Montfoort, A., *Surface Sci.* **4**, 396 (1966).
3. Foger, K., and Anderson, J. R., *J. Catal.* **54**, 318 (1978).
4. Boudart, M., Aldag, A. W., Ptak, L. D., and Benson, J. E., *J. Catal.* **16**, 11,35 (1968).
5. Karnaukhov, A. P., *Kinet. Katal.* **12**(6), 1520 (1971).
6. Paltovak, O. M., Boronin, V. S., and Mitrofanova, A. N., *in* "Proceedings, 4th International Congress on Catalysis, Moscow, 1968" (B. A. Kazansky, Ed.), p. 276. Alder, New York.
7. Baker, R. T. K., Prestridge, E. B., and Garten, R. L., *J. Catal.* **56**, 390 (1979).
8. Chen, M., and Schmidt, L. D., *J. Catal.* **55**, 348 (1978).
9. Avery, N. R., and Sanders, J. V., *J. Catal.* **18**, 129 (1970).
10. Sawruk, S., Rohrman, A., Jr., and Kokotailo, G., *J. Catal.* **40**, 379 (1975).
11. Nakamura, M., Yamada, M., and Amano, A., *J.Catal.* **39**, 125 (1975).
12. Chen, M., and Schmidt, L. D., *J. Catal.* **56**, 198 (1979).
13. Fuentes, S., and Figueras, F., *J. Catal.*, in press.
14. Yacamán, M. J., and Ocaña, T., *Phys. Status Solidi. A* **47**, 571 (1977).
15. Bartholomew, C. H., and Boudart, M., *J. Catal.* **25**, 173 (1972).
16. Hirsch, P. B., Howie, A., Pashley, R. B., Nicholson, W., and Whelon, M. J., "Electron Microscopy of Thin crystals." Butterworths, London, 1965.
17. Freeman, L. A., Howie, A., and Treacy, M. M., *J. Microsc.* **111**, 165 (1977).
18. Ino, S., *J. Phys. Soc. Japan* **21**, 346 (1966).
19. Larroque, P., and Brieu, M., *Acta Crystallogr. A* **34**, 853 (1978).
20. Yacamán, M. J., and Domínguez E., J. M., *Surface Sci.*, in press.
21. Domínguez E., J. M., and Yacamán, M. J., *J. Catal.*, in press.
22. Chu, Y. F., and Ruckenstein, E., *Surface Sci.* **67**, 517 (1977).
23. Bett, J. A., Kinoshita, K., and Sonehart, P., *J. Catal.* **35**, 307 (1974).
24. Henning, G. R., *in* "Chemistry and Physics of Carbon" (P. L. Walker, Jr., Ed.), Vol. 2. Dekker, New York, 1966.
25. Tomita, A., and Tamai, Y., *J. Phys. Chem.* **78**, 2254 (1974).